ISSN 1674-1056
http://cpb.iphy.ac.cn
http://iopscience.iop.org/cpb
中国物理 B
Chinese Physics
中国物理 Chinese Physics B

High-frequency enhancement-mode millimeterwave AlGaN/GaN HEMT with an f_T/f_{max} over 100 GHz/200 GHz

Sheng Wu(武盛), Minhan Mi(宓珉瀚), Xiaohua Ma(马晓华), Ling Yang(杨凌), Bin Hou(侯斌), and Yue Hao(郝跃)
Citation: Chin. Phys. B, 2021, 30 (**8**): 087102. DOI: 10.1088/1674-1056/ac04a5
Journal homepage: http://cpb.iphy.ac.cn; http://iopscience.iop.org/cpb

What follows is a list of articles you may be interested in

Analysis on degradation mechanisms of normally-off p-GaN gate AlGaN/GaN high-electron mobility transistor

Si-De Song(宋思德), Su-Zhen Wu(吴素贞), Guo-Zhu Liu(刘国柱), Wei Zhao(赵伟), Yin-Quan Wang(王印权), Jian-Wei Wu(吴建伟), and Qi He(贺琪)
Chin. Phys. B, 2021, 30 (**4**): 047103. DOI: 10.1088/1674-1056/abccba

Characterization and optimization of AlGaN/GaN metal-insulator semiconductor heterostructure field effect transistors using supercritical CO_2/H_2O technology

Meihua Liu(刘美华), Zhangwei Huang(黄樟伟), Kuan-Chang Chang(张冠张), Xinnan Lin(林信南), Lei Li(李蕾), and Yufeng Jin(金玉丰)
Chin. Phys. B, 2020, 29 (**12**): 127101. DOI: 10.1088/1674-1056/abb22f

In-situ SiN combined with etch-stop barrier structure for high-frequency AlGaN/GaN HEMT

Min-Han Mi(宓珉瀚), Sheng Wu(武盛), Ling Yang(杨凌), Yun-Long He(何云龙), Bin Hou(侯斌), Meng Zhang(张濛), Li-Xin Guo(郭立新), Xiao-Hua Ma(马晓华), Yue Hao(郝跃)
Chin. Phys. B, 2020, 29 (**4**): 047104. DOI: 10.1088/1674-1056/ab7746

Effects of post-annealed floating gate on the performance of AlGaN/GaN heterostructure field-effect transistors

Peng Cui(崔鹏), Zhao-Jun Lin(林兆军), Chen Fu(付晨), Yan Liu(刘艳), Yuan-Jie Lv(吕元杰)
Chin. Phys. B, 2017, 26 (**12**): 127102. DOI: 10.1088/1674-1056/26/12/127102

Modified model of gate leakage currents in AlGaN/GaN HEMTs

Yuan-Gang Wang(王元刚), Zhi-Hong Feng(冯志红), Yuan-Jie Lv(吕元杰), Xin Tan(谭鑫), Shao-Bo Dun(敦少博), Yu-Long Fang(房玉龙), Shu-Jun Cai(蔡树军)
Chin. Phys. B, 2016, 25 (**10**): 107106. DOI: 10.1088/1674-1056/25/10/107106

High-frequency enhancement-mode millimeterwave AlGaN/GaN HEMT with an f_T/f_{max} over 100 GHz/200 GHz*

Sheng Wu(武盛), Minhan Mi(宓珉瀚)†, Xiaohua Ma(马晓华), Ling Yang(杨凌), Bin Hou(侯斌), and Yue Hao(郝跃)

Key Laboratory of Wide Band-Gap Semiconductor Materials and Devices, School of Microelectronics, Xidian University, Xi'an 710071, *China*

(Received 6 April 2021; revised manuscript received 1 May 2021; accepted manuscript online 25 May 2021)

Ultra-thin barrier (UTB) 4-nm-AlGaN/GaN normally-off high electron mobility transistors (HEMTs) having a high current gain cut-off frequency (f_T) are demonstrated by the stress-engineered compressive SiN trench technology. The compressive *in-situ* SiN guarantees the UTB-AlGaN/GaN heterostructure can operate a high electron density of 1.27×10^{13} cm^{-2}, a high uniform sheet resistance of 312.8 Ω/□, but a negative threshold for the short-gate devices fabricated on it. With the lateral stress-engineering by full removing *in-situ* SiN in the 600-nm SiN trench, the short-gated (70 nm) devices obtain a threshold of 0.2 V, achieving the devices operating at enhancement-mode (E-mode). Meanwhile, the novel device also can operate a large current of 610 mA/mm and a high transconductance of 394 mS/mm for the E-mode devices. Most of all, a high f_T/f_{max} of 128 GHz/255 GHz is obtained, which is the highest value among the reported E-mode AlGaN/GaN HEMTs. Besides, being together with the 211 GHz/346 GHz of f_T/f_{max} for the D-mode HEMTs fabricated on the same materials, this design of E/D-mode with the realization of f_{max} over 200 GHz in this work is the first one that can be used in Q-band mixed-signal application with further optimization. And the minimized processing difference between the E- and D-mode designs the addition of the SiN trench, will promise an enormous competitive advantage in the fabricating costs.

Keywords: ultra-thin barrier (UTB), AlGaN/GaN, *in-situ* SiN, stress-engineering, enhancement-mode, mixed-signal applications

PACS: 71.55.Eq, 73.20.–r, 73.50.–h **DOI:** 10.1088/1674-1056/ac04a5

1. Introduction

Due to the high breakdown electric field and electron mobility, AlGaN/GaN high electron mobility transistors (HEMTs) release greater advantages in high-power radio-frequency (RF) applications over Si- and GaAs-based devices from L (1 GHz–2 GHz) band to W (75 GHz–110 GHz) band.[1,2] However, the most high-frequency devices reported have been in depletion mode (D-mode), which would need a more passive circuit to fit the electrical supply, inducing significant losses.[3] Therefore, normally-off devices do not only enable circuit simplicity reducing the RF-loses benefit for high-frequency operation but also be preferred in power switching for safety and reduced power consumption. Finally, there is a demand for E/D-mode logic for digital circuits and mixed-signal applications.[3]

The technology of the E-mode GaN HEMTs has been fully studied.[4–6] In the past, the challenges of the GaN-based E-mode HEMTs are mainly focused in the trade-off between large output current and positive threshold.[6] Although a large current of 1.9 A/mm with a threshold of 0.8 V and a threshold of 4.6 V with a low current of 4.4 mA/mm have been achieved respectively in Refs. [7,8], there is few people can achieve the balance of these two parameters like the works in Ref. [9]. Besides, few peers have studied the RF-performances of the E-Mode HEMTs and tried to improve it, which has brought a lot of obstacles to the high-frequency applications of E-mode HEMTs. Thereby, it is necessary to achieve an E-mode HEMT with a great high-frequency performance to suit the mixed-signal applications.

In this work, enhancement-mode (E-mode) UTB AlGaN/GaN HEMT with a large drain current and an excellent frequency characteristic is demonstrated, on the same material, which has been proved to be reliable and stable.[10] In the UTB AlGaN/GaN heterostructure, a 20-nm high strained *in-situ* SiN cap layer is adopted to improve the polarization of the material, enhancing the electron density, and guaranteeing the output level as a normal industrial one. Meanwhile, the proper-sized trench around the gate makes the device maintain a positive threshold, but the influence of the stressed SiN is not completely released by the removal of the SiN. The phenomenon of the trench-size influencing the threshold characteristics of the E-mode devices can be observed, which is similar to that of the gate length influencing tendency observed in the D-mode ones without the trench. It is worthy to note

*Project supported by the National Key Research and Development Program of China (Grant No. 2020YFB1804902), the National Natural Science Foundation of China (Grant No. 61904135), the China Postdoctoral Science Foundation (Grant Nos. 2018M640957 and BX20200262), and the Natural Science Foundation of Shaanxi Province, China (Grant No. 2020JQ-316).

†Corresponding author. E-mail: miminhan@qq.com

© 2021 Chinese Physical Society and IOP Publishing Ltd

that the device does not only do not reduce its output current too much, about 40%, but it also made the devices obtain an excellent frequency of 128 GHz/255 GHz for E-mode. Moreover, the new obtained frequency is the highest value in the E-mode AlGaN/GaN HEMTs that have been reported. Most of all, the simpler process fabrication and smaller process differences between the E/D-modes make the integration of the E/D-modes easier to approve, promising its great potential in high-frequency digital circuits and mixed-signal applications.

2. Material growth and device fabrication

Figure 1 exhibits the schematic cross-section of the proposed UTB-AlGaN/GaN HEMT. The AlGaN/GaN heterostructure adopted in this work was epitaxially grown on 3-inch (1 inch = 2.54 cm) SiC based on metal–organic chemical vapor deposition (MOCVD), and the epitaxial heterostructure consists of a 20-nm *in-situ* SiN cap layer, a 4-nm UTB $Al_{0.2}Ga_{0.8}N$ barrier, and a semi-insulating GaN buffer. It is worthy to note that the electron density and mobility of the as-grown material were measured to be 1.26×10^{13} cm^{-2} and 1675 cm^2/V·s, while before the tensile stress high as 2.35 GPa carried from the compressive SiN, those are 7.23×10^{11} cm^{-2} and 2051 cm^2/V·s respectively. These improvements of the material might be related to the charge neutralizing[11] and stress-induced polarization enhancement.[10] The device fabrication process began with the removal of the *in-situ* SiN on the Ohmic region carried by the F-based inductively coupled plasma reactive ion etching (ICP-RIE). Then the metal Ti/Al/Ni/Au stack was evaporated as Ohmic contact formation and rapid temperature annealing (RTP) was performed at 850 °C for 30 s in an N_2 atmosphere. After the F-based ICP-RIE, mesa isolation was formed by Cl-based ICP-RIE to remove the SiN attached out of the active region. The Ohmic contact resistance (R_C) of 0.5 Ω·mm was measured by the transfer line measurement. To distinguish the E-mode and D-mode devices, a recess trench was carried by the F-based ICP-RIE on *in-situ* SiN around the gate of the E-mode HEMT. After a 70-nm T-gate was fabricated on the devices, the novel E-mode HEMT was passivated by a SiN layer with a thickness of 50 nm, also deposited by plasma-enhanced chemical vapor deposition (PECVD).

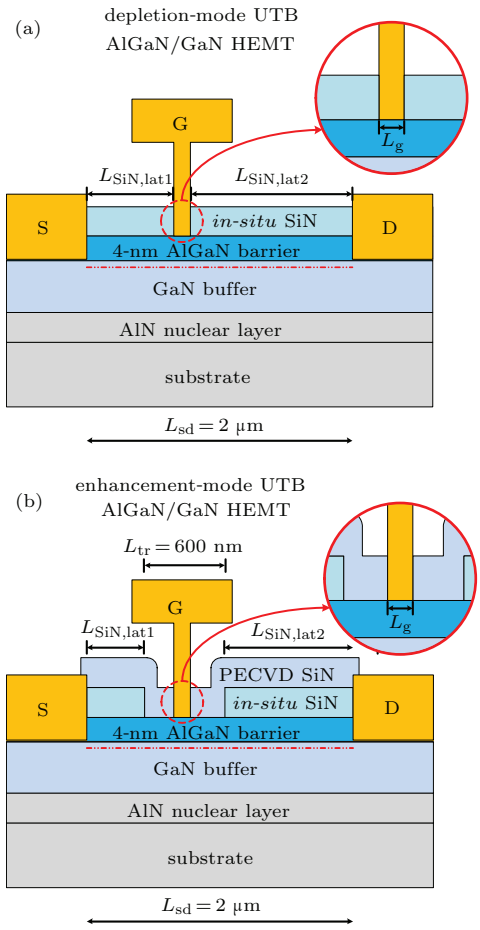


Fig. 1. Schematic drawing of UTB AlGaN/GaN D-HEMT and E-HEMT used in millimeter-wave applications: (a) schematic diagram of D-mode AlGaN/GaN HEMT and (b) schematic diagram of E-mode AlGaN/GaN HEMT.

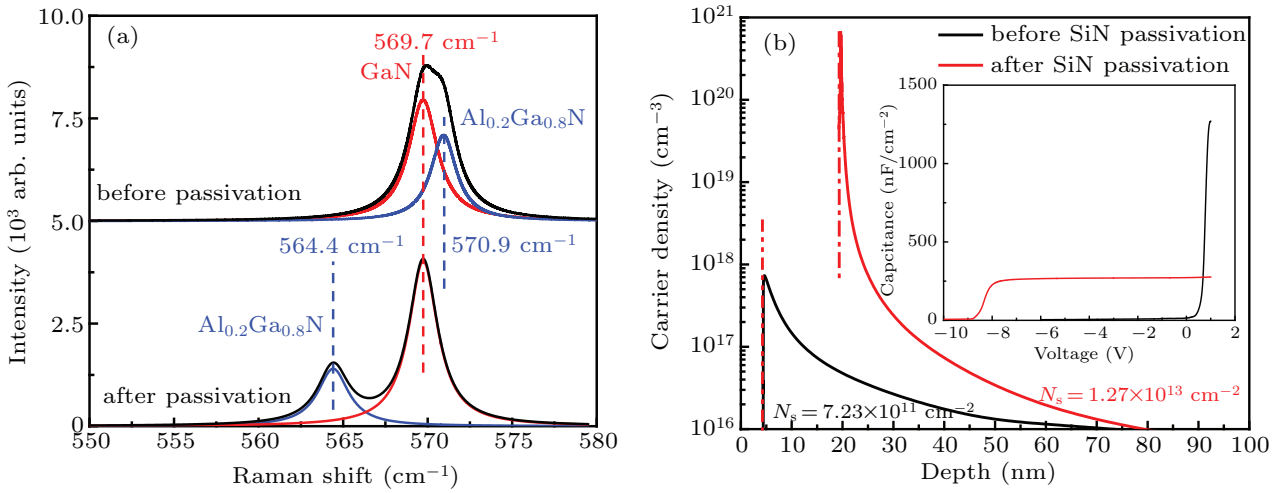


Fig. 2. (a) The Raman spectra probed with a 442-nm laser for the UTB AlGaN/GaN heterostructure and (b) the electron density extracted from *C–V* measurement before and after the SiN passivations.

To investigate the effect of compressive *in-situ* SiN passivation, a Raman spectra probed with a 442-nm laser were carried out on the fabricated samples respectively before and after the passivation. Under the premise of accurate focusing, due to the weak penetrability of the long-wavelength Raman laser, we can collect the frequency information near the surface of the material, which includes the $E_{2(\mathrm{high})}$ peaks of AlGaN and GaN.[12,13] From the Raman result, both the two materials can be observed a series of peaks near 568 cm^{-1} representing the $E_{2(\mathrm{high})}$ peaks of GaN, whatever the strained SiN was covered or not. Before the SiN passivation, the Raman peaks can be divided into two peaks whose FHWMs are similar, respectively located at 569.7 cm^{-1} and 570.9 cm^{-1}. However, with passivation of the high-compressive SiN, the material was observed two discrete peaks respectively at 564.4 cm^{-1} and 569.7 cm^{-1}. According to the delta and coefficient[14] of the frequency shift, a high as 2.35-GPa tensile stress was determined to carry on the AlGaN barrier for the novel devices, which can be enough to enhance the polarization of the material, inducing an improvement of carrier density shown in Fig. 2(b).

3. Results and discussion

Figure 3 shows the DC output and transfer characteristics of the fabricated E-mode AlGaN/GaN HEMT. A large maximum I_{D} of 610 mA/mm and a high transconductance as 393 mS/mm are obtained for the devices, when the drain voltage bias set at $V_{\mathrm{ds}} = 10$ V, and those for the D-mode device are respectively 975 mA/mm and 424 mS/mm. The threshold voltage is measured stable at 0.2 V for the E-mode device with the trench size of 600 nm, while that of the D-mode device is measured as a result of −0.6 V. Meanwhile, the on-resistance of the two devices are respectively 2.1 Ω·mm and 4.6 Ω·mm, which are lower respectively than devices fabricated as E/D modes for conventional material. This is mainly related to the high stressor *in-situ* SiN fully (for D-mode) or partially (for E-mode) enhance the polarization of material in the access region, greatly reducing the parasitic resistance in the channel. Besides, the fabricated E-mode and D-mode devices both exhibit good pinch-off characteristics, and this is mainly benefited by the high aspect ratio of 18 (L_{g}/d, where d is the distance between the gate and channel and L_{g} is gate length).

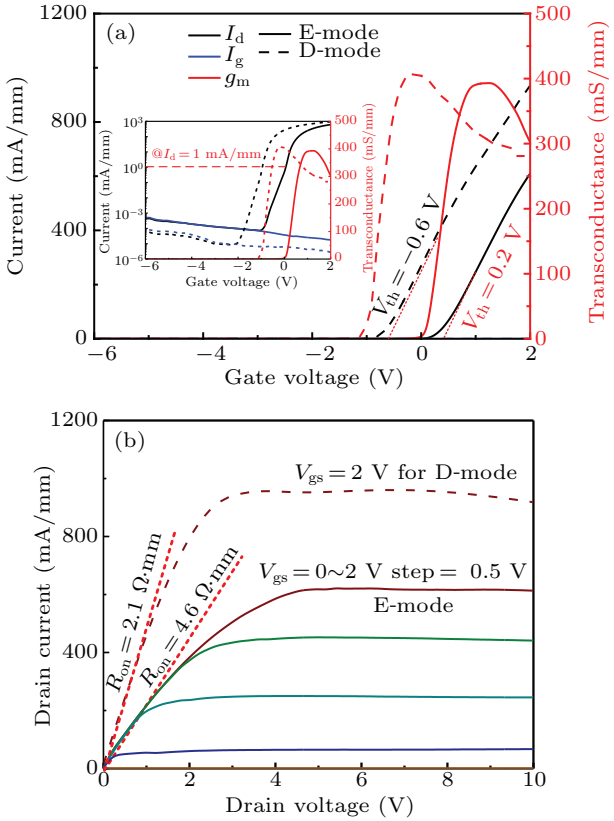


Fig. 3. The *I*–*V* measurement for E/D-modes UTB AlGaN/GaN HEMT: (a) transfer characteristics and (b) output characteristics. The solid line is the curves of E-mode HEMT, and the dashed line is the curves of D-mode HEMT. The colors of the curves respectively correspond to the drain current (I_{d}, black), gate current (I_{g}, blue), and the transconductance (g_{m}, red). The red dashed straight line in the inset is to indicate the threshold standard (@$I_{\mathrm{d}} = 1$ mA/mm) in semi-logarithmic coordinates.

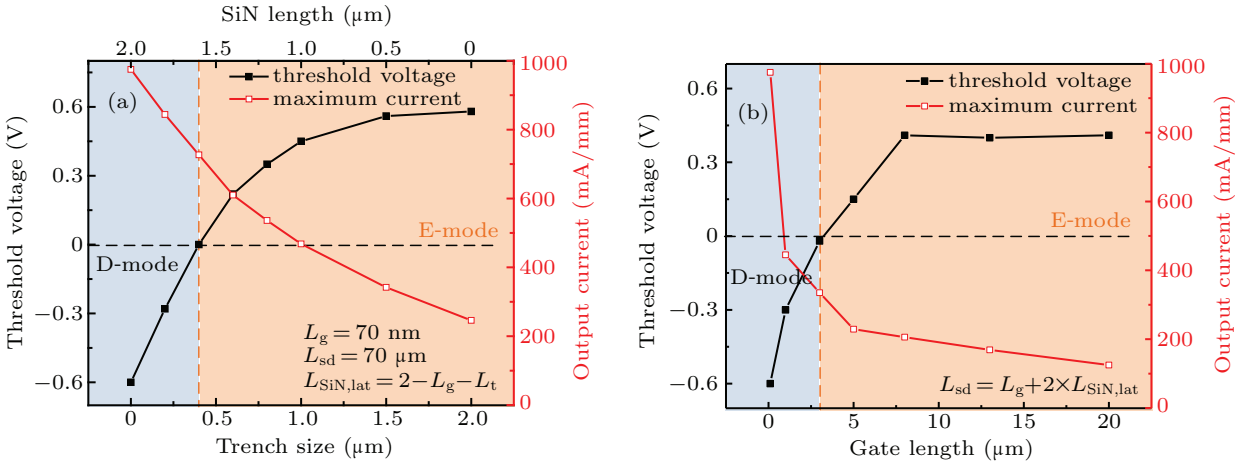


Fig. 4. The impact of structure sizes on the E/D modes UTB AlGaN/GaN HEMTs: (a) the impact of trench size in E-mode design and (b) the impact of gate length in D-mode design. The orange dashed lines are to distinguish the operating mode of the devices with these sizes in two types of design, and the black dashed line is used to mark the reference boundary between definitions of E-mode and D-mode.

Moreover, the threshold of two types of devices is related to the gate length (L_g) and trench size (L_{tr}). Figure 4 illustrates the phenomenon that V_{th} is changing with the size of two structures. With the increasing of L_g or trench size, the V_{th} of E/D-modes devices both are shifting-positive. Both two-type devices are related to the stressor being gradually separated away. The impact of the stress under the gate is depleted by the distance between two sides SiNs. Although the range affected by the stress from SiN side-wall edges can be determined as 2 μm–4 μm from the Fig. 4(b), the strength of the stress is also related to the size of the side SiN ($L_{SiN,lat}$). Therefore, the V_{th} for the trenched-device shift faster due to the decreasing $L_{SiN,lat}$ with L_{tr}, when compared to the full-gated devices with the constant $L_{SiN,lat} = 2$ μm (D-mode design, $L_{tr} = 0$ μm). Finally, the device with a trench-size of 600 nm was selected as the E-mode design because of the acceptable current losses and the achieving of normally-off.

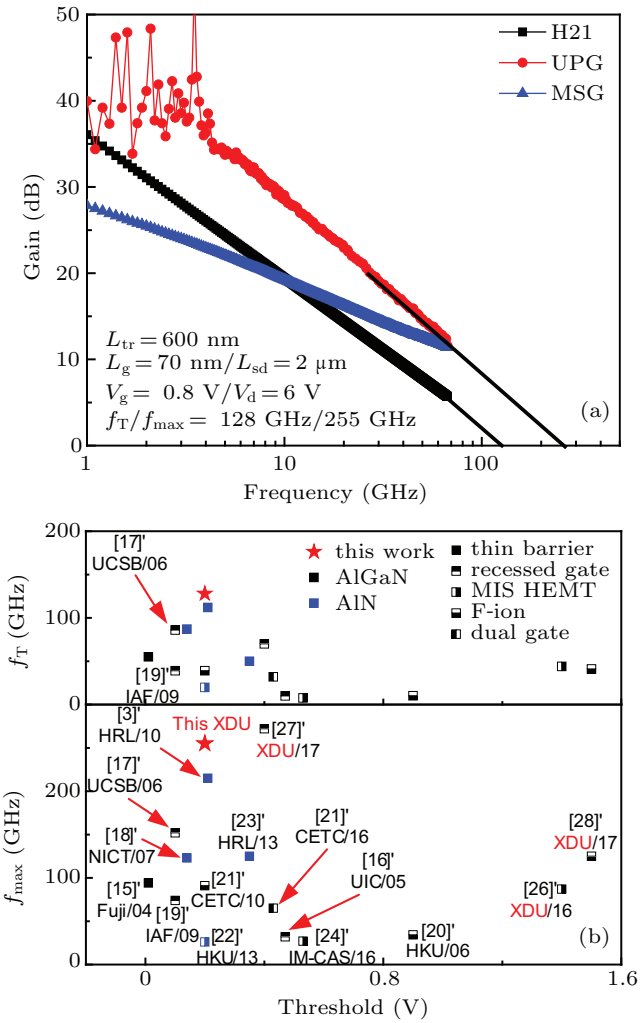


Fig. 5. RF performance of UTB AlGaN/GaN E-HEMT used in millimeter-wave applications: (a) small-signal RF performance and (b) summarisation of measured f_T and f_{max} in E-mode HEMT from recently reported state-of-art results.

The RF small-signal characteristics of the proposed E-mode HEMTs were obtained by a vector network analyzer with the step of 0.1 GHz from 100 MHz to 67 GHz during the on-wafer measurements. To subtract the influence of parasitic pad inductances and capacitances from the obtained small-signal parameters, on-wafer cold and hot FET techniques were adopted. Figure 5(a) shows Mason's unilateral gain (U) and current gain ($|H_{21}|^2$) against frequency for the fabricated E-mode AlGaN/GaN HEMTs, which are measured at V_{gs} of 0.8 V and V_{ds} of 6 V. By extrapolating the short circuit current gain (H_{21}) and the max stable gain (MSG) using −20-dB/dec slopes, f_T/f_{max} are 128 GHz/255 GHz. The values of f_T and f_{max} in the published E-mode HEMTs from other research teams are shown in Fig. 5(b).[3,15–28] The obtained value of f_T/f_{max} (128 GHz/255 GHz) is found to the highest-recorded result in the reported E-mode GaN HEMTs. As we all know that the f_{max} of the devices should be at least twice larger than the operating frequency in practical circuits. However, in the recent reported E-mode GaN devices, the values of f_{max} are rarely over 200 GHz. Therefore, being together with the 211 GHz/346 GHz of f_T/f_{max} for the D-mode HEMT fabricated on the same materials, this design of E/D-modes with the realization of f_{max} over 200 GHz in this work is the first one that can be used in Q-band mixed-signal application with further optimization.

4. Conclusion

The first E-mode AlGaN/GaN HEMT can be operating at a frequency over 100 GHz/200 GHz is demonstrated by the lateral stress-engineering on the *in-situ* SiN layer. The removal of the *in-situ* SiN in the trench region reduces a part of the stress-impact on electron density under the trench, making the material in this region suitable for the gate metal to obtain an E-mode device. Meanwhile, the *in-situ* SiN remaining outside the trench can continue to enhance the polarization of material, guaranteeing the R_{ch} does not affect the output current, on-resistance, and frequency characteristics too much. Compared with D-mode design, the output current, on-resistance, and frequency performances of E-mode HEMT are respectively degraded by 40%, 119%, and 26%. Due to the large aspect ratio of 18, the extremely thinned barrier can provide a strong control ability of the gate to the channel. Therefore, the device can operate a large $g_{m,ext}$ of 394 mS/mm and a large $g_{m,int}$ of 517 mS/mm, obtaining a promising frequency of 128 GHz/255 GHz for an E-mode AlGaN HEMTs. Most of all, the difference between the E/D-modes HEMT in this material with high stressor *in-situ* SiN is only the introducing of the trench or not. In other words, this technology can get more reliable mixed-signal applications in high-frequency, greatly simplifying the circuit cost and integration of the applications.

References

[1] Chung J W, Hoke W E, Chumbes E M and Palacios T 2010 *Electron Dev. Lett.* **31** 195

[2] Wu S B, Gao J F, Wang W B and Zhang J Y 2016 *Trans. Electron Dev.* **63** 3882

[3] Corrion A L, Shinohara K, Regan D, Milosavljevic I, Hashimoto P, Willadsen P. J, Schmitz A, Wheeler D C, Butler C M, Brown D, Burnham S D and Micovic M 2010 *Electron Dev. Lett.* **31** 1116

[4] Hu Z Y, Yue Y Z, Zhu M D Zhu, Song B, Ganguly S, Bergman J, Jena D and Xing H L 2014 *Appl. Phys. Express* **7** 031002

[5] Han P C, Wu C H, Ho Y H, Yan Z Z and Chang E Y 2019 *Proceedings of the* 31*st Intenational Symposium on Power Semiconductor Device & ICs*, May 19–23, 2019, Shanghai, China, p. 427

[6] Wen Y H, He Z Y, Li J L, Luo R H, Xiang P, Deng Q Y, Xu G N, Shen Z, Wu Z S, Zhang B J, Jiang H, Wang G and Liu Y 2011 *Appl. Phys. Lett.* **98** 072108

[7] Wan R H, Liu X, Lian C X, Gao X, Guo S P, Snider G, Fay P, Jena D and Xing H L 2010 *Electron Dev. Lett.* **31** 1383

[8] Cheng Z, Zhang Y, Zhang L, Zhao Y B, Wang J X and Li J M 2016 13*th China International Forum on Solid State Lighting: International Forum on Wide Bandgap Semiconductors*, January 5–12, 2017, Beijing, China, p. 72

[9] Huang S, Liu X Y, Wang X H, Kang X W, Zhang J H, Bao Q L, Wei K, Zheng Y K, Zhao C, Gao H W, Sun Q, Zhang Z F and Chen K J 2016 *Electron Dev. Lett.* **37** 1617

[10] Derluyn J, Boeykens S, Cheng K, Vandersmissen R, Das J, Ruythooren W, Degroote S, Leys M R, Germain M and Borghs G 2005 *J. Appl. Phys.* **98** 054501

[11] Dogmus E, Kabouche R, Linge A, Okada E, Zegaoui M and Medjdoub F 2017 *Phys. Status Solidi A* **214** 1600797

[12] Cheng W C, Lei S Q, Li W M, Zhao F, Chan M and Yu H Y 2019 *Electron Devices Technology and Manufacturing Conference*, March 12–15, 2019, Singapore, p. 19739002

[13] Cheng W C, Fang T, Lei S Q, Zhao Y L, He M H, Chan M, Xia G R, Zhao F and Yu H Y 2019 *IEEE International Conference on Electron Devices and Solid-State Circuits*, July 12–14, 2019, Xi'an China, p. 18864091

[14] Kuball M 2001 *Surf. Interface Anal.* **31** 987

[15] Endoh A, Yamashita Y, Ikeda K, Higashiwaki M, Hikosaka K, Matsui T, Hiyamizu S and Mimura T 2004 *Jpn. J. Appl. Phys.* **43** 2255

[16] Lanford W B, Tanaka T, Otoki Y and Adesida I 2005 *Electron. Lett.* **7** 449

[17] Palacios T, Chakraborty C S Sus, Chakraborty A, Keller S, DenBaars S P and Mishra U K 2006 *Electron Dev. Lett.* **6** 428

[18] Higashiwaki M, T Mimura T and Matsui T 2007 *Trans. Electron Dev.* **54** 1566

[19] Maroldt S, Haupt C, Pletschen W, Muller S, Quay R, Ambacher O, Schippel C and Schwierz F 2009 *Jpn. J. Appl. Phys.* **48** 04C083

[20] Cai Y, Zhou Y G, Chen K J and Lau K M 2005 *Electron Dev. Lett.* **26** 435

[21] Feng Z H, Zhou R, Xie S Y, Yin J Y Fang J X, Liu B, Zhou W, Chen K J and Cai S J 2010 *Electron Dev. Lett.* **31** 1386

[22] Huang T D, Liu Z J, Zhu X L Ma J, Lu X and Lau K M 2013 *Trans. Electron Dev.* **60** 3019

[23] Brown D F, Shinohara K, Corrion A L, Chu R M, Willianms A, Wong J C, Alvarado-Rodriguez I, Grabar R, Johnson M, Butler C M, Santos D, Burnham S D, Robinson J F, Zehnder D, Kim S J, Oh T C and Micovic M 2013 *Electron Dev. Lett.* **34** 111

[24] Huang S, Liu X Y, Zhang J H, Wei K, Liu G G, Wang X H, Zheng Y K, Liu H G, Jin Z, Zhao C, Liu C, Liu S H, Yang S, Zhang J C, Hao Y and Chen K J 2015 *Electron Dev. Lett.* **36** 754

[25] Gao T, Xu R, Kong Y C, Zhou J J, Zhang K, Kong C, Peng D Q and Chen T S 2016 *Phys. Status Solidi A* **213** 1241

[26] Yang L, Mi M H, Hou B, Zhu J J, Zhang M, Lu Y, He Y L, Zhu Q, Chen L X, Zhou X W, Lv L, Cao Y R, Ma X H and Hao Y 2017 *Trans. Electron Dev.* **64** 4057

[27] Mi M H, Ma X H, Yang L, Hou B, Zhu J J, He Y L, Zhang M, Wu S and Hao Y 2017 *Appl. Phys. Lett.* **111** 173502

[28] Hou B, Ma X H, Yang L, Zhu J J, Zhu Q, Chen L X, Mi M H, Zhang H S, Zhang M, Zhang P, Zhou X W and Hao Y 2017 *Appl. Phys. Express* **7** 076501